Development 129, 5301-5312 (2002)
Printed in Great Britain © The Company of Biologists Limited 2002
DEV20016

DEVELOPMENT AND DISEASE

Sonic hedgehog regulates proliferation and differentiation of mesenchymal cells in the mouse metanephric kidney

Jing Yu, Thomas J. Carroll and Andrew P. McMahon*

Department of Molecular and Cellular Biology, 16 Divinity Avenue, Harvard University, Cambridge MA 02138, USA
*Author for correspondence (e-mail: amcmahon@mcb.harvard.edu)

Accepted 12 August 2002

SUMMARY

Signaling by the ureteric bud epithelium is essential for survival, proliferation and differentiation of the metanephric mesenchyme during kidney development. Most studies that have addressed ureteric signaling have focused on the proximal, branching, ureteric epithelium. We demonstrate that sonic hedgehog is expressed in the ureteric epithelium of the distal, non-branching medullary collecting ducts and continues into the epithelium of the ureter – the urinary outflow tract that connects the kidney with the bladder. Upregulation of patched 1, the sonic hedgehog receptor and a downstream target gene of the signaling pathway in the mesenchyme surrounding the distal collecting ducts and the ureter suggests that sonic hedgehog acts as a paracrine signal. In vivo and in vitro analyses demonstrate that sonic hedgehog promotes mesenchymal cell proliferation, regulates the timing of differentiation of smooth muscle progenitor cells, and sets the pattern of mesenchymal differentiation through its dose-dependent inhibition of smooth muscle formation. In addition, we also show that bone morphogenetic protein 4 is a downstream target gene of sonic hedgehog signaling in kidney stroma and ureteral mesenchyme, but does not mediate the effects of sonic hedgehog in the control of mesenchymal proliferation.

Key words: Kidney, Sonic hedgehog, *Shh*, Proliferation, Smooth muscle, Mouse, Ureter, Hydroureter

INTRODUCTION

The metanephric kidney forms through reciprocal inductive interactions between the ureteric bud epithelium and the metanephric mesenchyme. The ureteric bud, an outgrowth of the Wolffian (or mesonephric) duct, invades the metanephric blastema and arborizes to form the collecting duct system within the kidney and the ureter (the latter connects the collecting duct network to the bladder). The metanephric mesenchyme, however, can adopt one of several fates, including epithelial renal vesicles, stroma or smooth muscle, in response to local signaling (Aufderheide et al., 1987; Herzlinger et al., 1992; Matsuno et al., 1984; McHugh, 1995; Saxen, 1987; Tacciuoli et al., 1975). Smooth muscle forms only from the mesenchyme surrounding the pelvis and the ureter, and is essential for the evacuation of urine. Regional or extensive failure of differentiation of the ureteral mesenchyme into muscular tissue is one of the major causes of congenital ureteral stricture (Tanagho, 1981). The resulting deficiency in urine transport causes atrophy of kidney parenchyma (Gillenwater, 1992).

The kidney is a classic model for the study of epithelial-mesenchymal interactions. The ureteric bud is essential for metanephric mesenchyme survival (Grobstein, 1953; Grobstein, 1955), and the metanephric mesenchyme is required for the growth and branching of the ureteric bud (Ekblom, 1992; Erickson, 1968; Grobstein, 1953; Grobstein, 1955). The developmental roles (if any) of the distal collecting ducts and the ureteric epithelium are unknown. Because smooth muscle forms adjacent to these regions, it seems likely that these tissues might regulate smooth muscle development.

Sonic hedgehog (*Shh*), a Drosophila *Hedgehog* (*Hh*) homolog, is expressed in the urothelium (Bitgood and McMahon, 1995; Karavanova et al., 1996) (this study). *Shh* has previously been shown to be involved in cell survival, proliferation, differentiation and pattern formation in various embryonic tissues (for reviews, see Ingham and McMahon, 2001; McMahon et al., 2002). Interestingly, *Shh* is located on human chromosome 7q36; deletions within this region, which may include *Shh*, are associated with kidney defects such as hydroureter (Lurie et al., 1990; Nowaczyk et al., 2000). Mutations in the *Shh* signaling pathway have been linked to renal anomalies in humans such as the VACTERL syndrome (Kim et al., 2001). In the mouse, removal of *Shh* generates a spectrum of defects (reviewed by McMahon et al., 2002), including kidney hypoplasia (A. P. M., unpublished). However, deciphering the possible role of *Shh* in kidney development directly in *Shh* mutants is hindered by the fusion of the paired

kidney primordia, a secondary consequence of midline defects in early somite stage embryos (A. P. M., unpublished). To address the role of *Shh* in kidney development, we have developed a conditional loss of function genetic approach that removes Shh signaling from the kidney primordium. These studies indicate that *Shh* is a crucial paracrine factor for the control of proliferation and differentiation in the subjacent mesenchyme that underlies the urothelium.

MATERIALS AND METHODS

HoxB7/Cre transgenic lines and generation of kidney specific mutants in Shh signaling

A cDNA encoding P1 phage integrase, Cre, was cloned into a vector containing a 1.3 kb *HoxB7* enhancer/promoter (Kress et al., 1990) and a human growth hormone (HGH) mini-gene (Chaffin et al., 1990), which provides introns and a poly-adenylation signal for efficient translation. Transgenic mice were generated by pronuclear injection and identified on Southern blots using *HGH* as a probe. Four founder males were identified that contained the transgene. Each transgenic male was crossed to females carrying the *ROSA 26* (*ROSA*) reporter allele (Zambrowicz et al., 1997). Kidneys were dissected at E12.5 and analyzed for expression of *lacZ* as previously described (Oberdick et al., 1994). Two of the four males tested (lines 5 and 13) expressed *lacZ* gene in the predicted pattern. Both males were crossed to Swiss webster (SW) females, and male offspring were genotyped via Southern hybridization. F_1 transgenic males were crossed to ROSA reporter mice and analyzed for *lacZ* expression. Offspring from line 5 showed mosaic expression, while those from line 13 showed even and robust expression. All further analysis was performed with offspring from line 13.

To further characterize the expression of *HoxB7/Cre*, lines were established that were transgenic for both *HoxB7/Cre* and either the *ROSA* or *Z/AP* reporter alleles (Lobe et al., 1999). Males carrying both *HoxB7/Cre* and one of the reporter transgenes were crossed to SW females and embryos were dissected at 24-hour intervals from E9.5 to P1. Either whole embryos (E9.5-E11.5) or dissected urogenital systems (E12.5-P1) were analyzed for *lacZ* (ROSA) or *lacZ* and alkaline phosphatase (Z/AP) expression according to Lobe et al. (Lobe et al., 1999). For the Z/AP embryos, salmon galactoside (Biosynth) was used as the β-galactosidase substrate. For histology, processed kidneys were post-fixed in 4% paraformaldehyde, embedded in paraffin wax and sectioned at 6 um.

The *HoxB7/Cre* mice were mated to $Shh^{n/+}$ mice (St-Jacques et al., 1998) to generate *HoxB7/Cre*, $Shh^{n/+}$ males. These males were mated to homozygous *Shh* conditional females ($Shh^{c/c}$) (Dassule et al., 2000) to generate *HoxB7/Cre*, $Shh^{c/n}$ progeny in which Shh signaling was specifically removed from the kidney urothelium. These kidneys are referred to as '*Shh* mutant kidneys' in the text.

Histological, in situ, histochemical and immunological analysis of kidneys

Kidneys were fixed in 4% paraformaldehyde at 4°C, dehydrated through a graded ethanol series, embedded in paraffin wax and sectioned at 6 μm (embryonic and newborn kidneys) or 7 μm (adult kidneys). Sections were stained with Hematoxylin and Eosin for histological analysis. In situ hybridization with ^{35}S-labeled probes was performed according to Wilkinson et al. (Wilkinson et al., 1987a; Wilkinson et al., 1987b), with minor modifications for the *Shh* probe (the hybridization temperature was reduced from 55°C to 50°C, and the washing temperature from 65°C to 60°C). To assay for β-galactosidase activity on sections, tissues were fixed in 2% paraformaldehyde for 50 minutes at 4°C, washed with PBS extensively, cryoprotected in 30% sucrose overnight and embedded in OCT. Cryosections (12 μm) were prepared and stained with *X-gal* according to the protocol of Oberdick et al. (Oberdick et al., 1994). Images were captured with a JVC KY-F70 digital camera on a Leitz DMRD microscope or by a Nikon digital camera DXM1200 on a Nikon SMZ1500 stereoscope.

For immunohistochemistry and immunofluorescence, paraffin wax embedded sections were dewaxed in xylenes and rehydrated through a graded ethanol series. Slides were microwaved for 15 minutes in 1 mM Tris-HCl (pH 8.0), 5 mM EDTA to unmask antigens. Sections were blocked in 2% sheep serum in PBS+0.1% Triton X-100 for 30 minutes. Endogenous peroxidase activity was quenched by incubating sections in 3% H_2O_2 for 10 minutes when peroxidase-conjugated secondary antibodies were used. The sections were then incubated with any of the following: monoclonal anti-smooth muscle α-actin antibody (1:2000, Sigma), biotin-conjugated *Dolichos bifloris* agglutinin (DBA) (1:200, Sigma) or polyclonal anti-phospho-histone H3 antibodies (1:50, Upstate Biotechnology) at 4°C overnight. Alexa 568-conjugated anti-mouse IgG (Molecular probes), Alexa 568-conjugated anti-rabbit IgG (Molecular probes) or Alexa 488-conjugated Streptavidin (Molecular probes) were used for immunofluorescent detection of the binding of the primary reagents. Nuclei were counterstained with DAPI. Sections were mounted in Vectashield mounting media (Vector laboratories) and visualized with a Zeiss LSM510 Axioplan 2 confocal microscope. Frozen sections stained with *X-gal* were post-fixed with 4% paraformaldehyde for 20 minutes, and stained with antibodies as above. For immunohistochemistry, peroxidase-conjugated anti-mouse IgG (Jackson ImmunoResearch) was used as the secondary antibody and its binding was visualized by histochemical staining in 3,3′-Diaminobenzidine (DAB) (Sigma). These sections were counterstained with Methyl Green, dehydrated and mounted in Permount mounting media (Fisher). Images were collected with a JVC KY-F70 digital camera on a Leitz DMRD microscope. Mitotic indices were calculated as the percentage of nuclei that were phospho-histone H3-positive in three to four adjacent sections in the same region of the proximal and distal ureter of *Shh* mutant and wild-type kidneys.

Calculation of kidney volume and the number of glomeruli

Glomeruli were identified by the presence of a Bowman's capsule. The volume of kidneys, of the cortex and of the medulla was measured according to Bertram et al. (Bertram et al., 1992) with the following modifications: 6 μm sections were stained with Hematoxylin and Eosin. The area of the tissue section of interest was measured with NIH image 1.62 and multiplied by the thickness to obtain the volume/section. The volume for each kidney is the sum of the volume for each section.

Ureteral mesenchymal cell primary culture and BrdU staining

Mesenchyme of E12.5 ureters was mechanically separated from the epithelium in sterile D-PBS (BioWhittaker) and cultured on fibronectin (Sigma)-coated Lab-Tek glass chamber slides (Nalge Nunc International) or fibronectin-coated 48-well tissue culture plates in DMEM supplemented with 10 ng/ml recombinant human TGFα (Sigma) and 50 ng/ml recombinant human FGF2 (R&D Systems). No epithelial pieces were observed in the culture. Thus, there was no major contamination of urothelium in the ureteral mesenchymal cell culture. Palmitic acid-modified recombinant human sonic hedgehog protein (N-SHH; Biogen), recombinant human noggin protein (Regeneron) and recombinant human bone morphogenetic protein 4 (BMP4, Genetics institute) were added to the culture as indicated in the text. Fresh culture media (50% volume change) was added every 2 days. At day 5, cells were labeled with 10 μM BrdU for 11 hours, and then processed according to the Becton Dickinson immunocytometry system manual. Cells were incubated with monoclonal anti-BrdU antibody (1:100, Becton Dickinson) at 4°C overnight, antibody binding was visualized by incubating with Alexa 568-conjugated anti-mouse IgG. Cells were counterstained with

DAPI, mounted in Vectashield mounting media and visualized with a Zeiss LSM510 Axioplan 2 confocal microscope.

RT-PCR

Total RNA was prepared from either freshly dissected ureteral mesenchyme or mesenchyme after 5 days of culture using an RNAqueous-4-PCR kit (Ambion). Samples were treated with DNaseI, and reverse transcribed according to the manual for 5′RACE for rapid amplification of cDNA ends (Invitrogen). To ensure the amount of PCR products reflects the abundance of the specific cDNA being amplified in total cDNA sample, the PCR cycle number for the linear amplification range was determined with the most abundant cDNA sample, and PCR with all samples was performed with the PCR cycle number identified. β-actin PCR primers and conditions were as specified in the QuantumRNA β-actin kit (Ambion). Primers for smooth muscle α-actin PCR were as described (Yang et al., 1999), and PCR conditions were 94°C for 1 minute, 55°C for 1 minute and 72°C for 1 minute for 35 cycles. Primers and conditions for *Bmp4* PCR were according to Oxburgh and Robertson (L. Oxburgh and E. J. Robertson, unpublished).

RESULTS

Hedgehog signaling in the developing mouse metanephric kidney

To first address the possible roles of Hedgehog signaling in the kidney and ureter, we examined expression of the two hedgehog genes known to be expressed during kidney organogenesis (Bitgood and McMahon, 1995; Valentini et al., 1997), sonic hedgehog (*Shh*) and Indian hedgehog (*Ihh*), as well as two potential targets, the hedgehog receptor patched 1 (*Ptch)* and bone morphogenetic protein 4 (*Bmp4*) (Dudley and Robertson, 1997) (Fig. 1). *Shh* expression was evident in the urothelium of the kidney and the presumptive ureter at E11.5 (data not shown). Within the kidney, *Shh* expression was restricted to the distal collecting ducts generated from the first branches of the ureteric bud (E14.5, Fig. 1A). No *Ihh* expression was detected in the kidney or the ureter at this time (E14.5, Fig. 1B), although a previous report using RT-PCR indicates that very low levels of transcripts may be present (Valentini et al., 1997). High levels of *Ptch* expression, a readout for cells responding to hedgehog signals, were observed in most layers of mesenchymal cells adjacent to the *Shh*-expressing epithelium of the collecting ducts and the ureter (E14.5, Fig. 1C). *Bmp4* was expressed in a similar domain to that of *Ptch* in addition to expression in the glomeruli (E14.5, Fig. 1D) (Dudley and Robertson, 1997; Miyazaki et al., 2000). At the newborn stage (NB), strong *Shh* expression was detected in the inner medullary collecting ducts, the renal pelvic epithelium (Fig. 1E and the inset), and the ureter epithelium (Fig. 1I). By contrast, *Ihh* expression was restricted to the nephronic epithelium in the outer medulla and the cortex (Fig. 1F) (Valentini et al., 1997), no expression was observed in the collecting ducts or ureter (Fig. 1F,J). The straight tubules are likely to be the major site of *Ihh* production at this stage. *Ptch* and *Bmp4* were both expressed in the mesenchyme of the medulla, and the renal pelvis (Fig. 1G,H). In the ureter, *Ptch* and *Bmp4* expression were restricted to a thin layer of mesenchymal cells immediately adjacent to the epithelium (Fig. 1K,L), and not in differentiated smooth muscle cells. The strong expression of *Ptch* in outer medullary stromal cells at the newborn stage is likely to be a direct response to Ihh signaling, whereas the upregulation of *Ptch* in mesenchymal cells underlying the collecting ducts and ureter suggests that these cells are targets of Shh signaling. Furthermore, the close correlation between the expression of *Ptch* and *Bmp4* in these regions is consistent with the

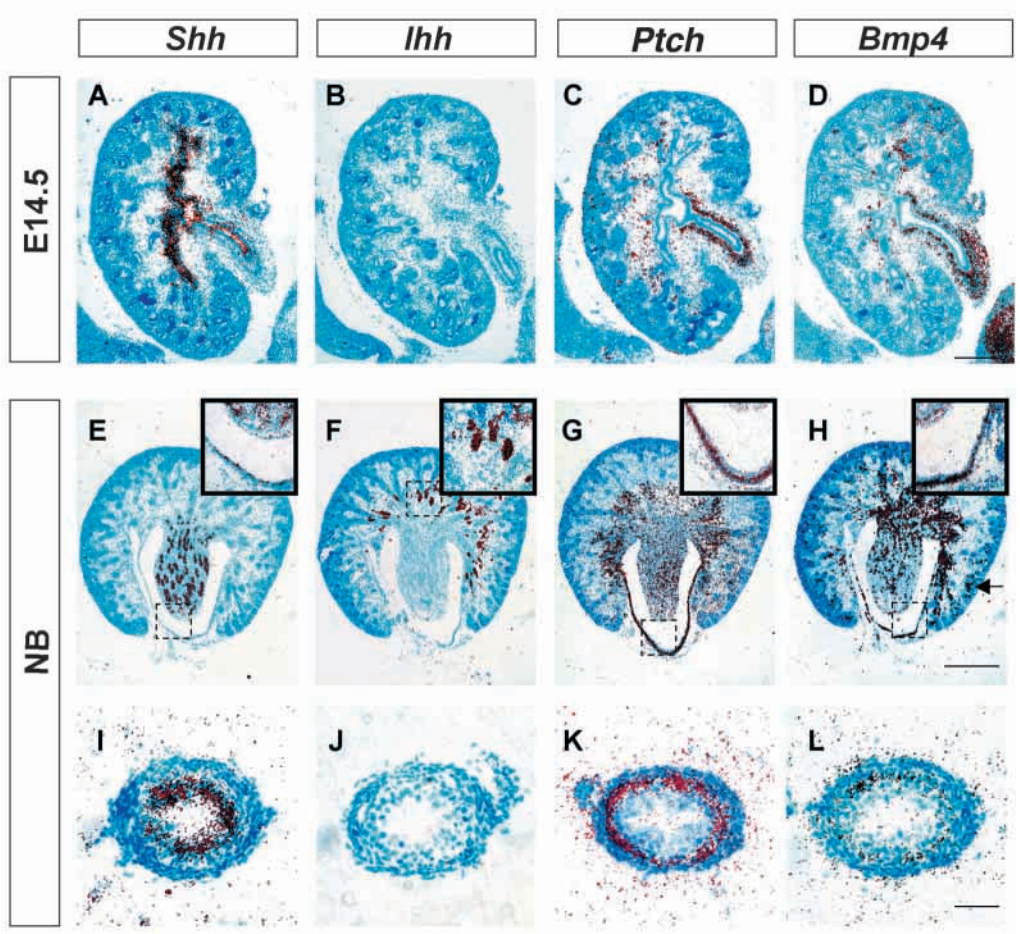

Fig. 1. Expression pattern of *Shh*, *Ihh*, *Ptch* and *Bmp4* in the prenatal and neonatal kidney and ureter. In situ hybridization with probes as indicated to stages as indicated. (A-D) Parasagittal sections of E14.5 kidney and ureter. Scale bar: 200 μm. (E-H) Coronal sections of the newborn kidney. Arrow in H indicates signals in glomeruli. Scale bar: 500 μm. (I-L) Cross-sections of the newborn ureter. Scale bar: 100 μm.

possibility that *Bmp4* expression may be regulated by Shh signaling.

The *HoxB7/Cre* transgenic mouse line

Analysis of the role of *Shh* in metanephric kidney formation in *Shh*-null mutants has been hindered by the midline defects in these animals, which causes the fusion of the two kidneys (J. Y., T. J. C. and A. P. M., unpublished). This problem was circumvented by generation of a mouse strain that drives Cre recombinase under the control of the *HoxB7* promoter/enhancer specifically within the mesonephric duct and its derivatives (the Wolffian duct, the collecting duct epithelium of the kidney and the ureteral epithelium). Cre activity could be detected with the *ROSA* reporter in the mesonephric duct as early as E9.5 (Fig. 2A), well before *Shh* expression initiates in the ureteric bud epithelium. HoxB7/Cre activity was detected throughout the ureteric bud from its initiation at E10.25 (Fig. 2B), and was clearly able to initiate recombination-mediated expression of the *ROSA* reporter gene in all ureteric bud epithelial cells by E12.5 (Fig. 2E,F). This is further confirmed by the *Z/AP* reporter (Fig. 2G-I). Consequently, intercrossing this transgenic line with one carrying a conditional *Shh* allele (Shh^{c}) (Dassule et al., 2000) that requires Cre-mediated recombination to remove essential sequences in exon2 – thereby generating a null allele (Shh^{n}) (Lewis et al., 2001) – allows the complete removal of Shh signal production prior to the normal activation of *Shh* in the ureteric epithelium.

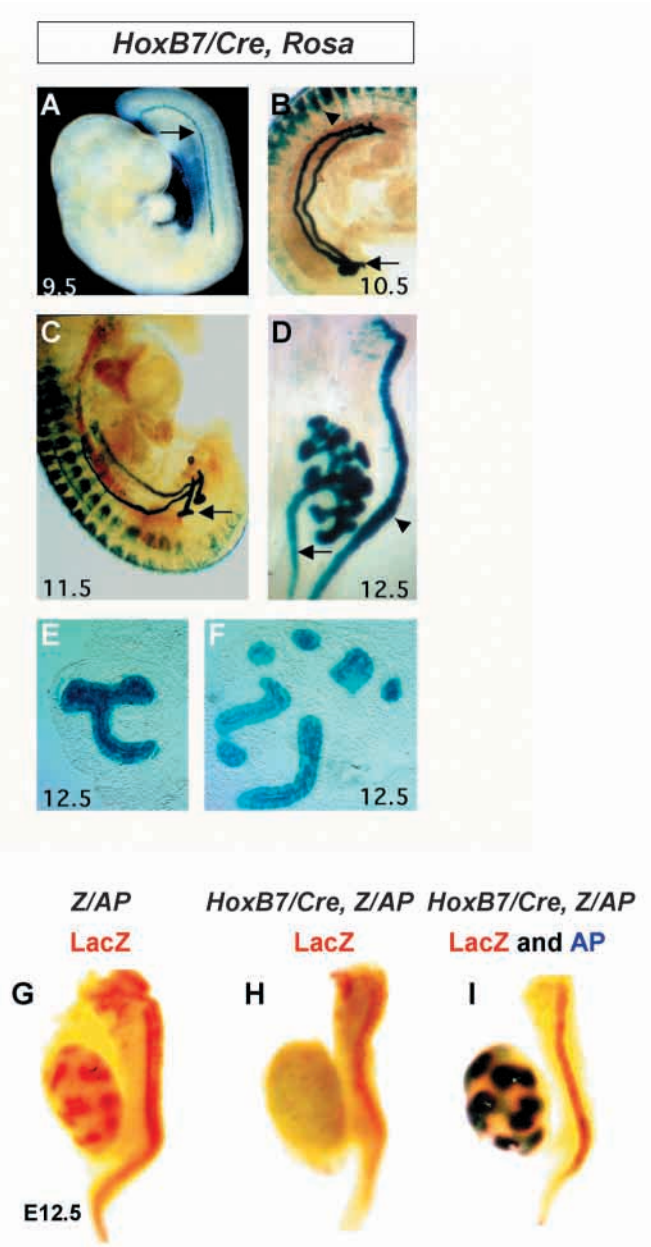

Removal of *Shh* activity from the urothelium causes renal hypoplasia, hydronephrosis and hydroureter

HoxB7/Cre, $Shh^{c/n}$ newborn pups were viable. However, their kidneys (hereafter referred to as '*Shh* mutant kidneys' for simplicity) were smaller and displayed a prominent hydroureter when compared with sex- and age-matched wild-type or heterozygous littermates (Fig. 3, compare 3A with 3B, and 3E with 3F). Hydroureter is usually more severe in the proximal region. Other than size, the gross anatomy of *Shh* mutant kidneys was not affected in newborn mutants (Fig. 3C,D). Consistent with this observation, the expression patterns of regional collecting duct markers, *Wnt15* and *Wnt7b*, were unaltered in mutants (data not shown). In addition to hydroureter (compare Fig. 3I with 3J), hydronephrosis (distention of the pelvis of a kidney) was detected in half of the adult mutant kidneys (5/10; Fig. 3H). Histological examination revealed that the hydronephric kidneys lost most of their inner medulla and the inner stripe of the outer medulla (Fig. 3G,H). Hydronephrosis in the mutant adult kidneys was probably secondary to the hydroureter, as severe hydronephrosis is always associated with severe hydroureter and no hydronephrosis was detected in newborn pups.

To determine whether *Shh* activity was effectively removed from the kidney, we examined *Ptch* expression (Fig. 4A-D). At E14.5, a time before significant differentiation of ureteral mesenchyme initiates (see below), *Ptch* expression was reduced to basal levels, indicating that no Shh signaling was occurring at this stage. Consistent with this observation, RT-PCR of *Shh* expression using exon 2 primers indicated a complete absence of a functional *Shh* transcript at E14.5 (data not shown).

Fig. 2. *HoxB7/Cre* reporter analysis. *HoxB7/Cre* mice were crossed to either Rosa (A-F) or Z/AP (G-I) reporter mice and subjected to histological staining to visualize β-galactosidase activity (A-F; G-I, red, *lacZ*) or alkaline phosphatase (I, blue, AP) activity. Ages of embryos are indicated. (A-D,G-I) Whole-mount views; (E-F) sections. (A) Mesonephric duct (arrow). (B) Mesonephric duct and onset of ureteric bud invasion into the metanephric mesenchyme (arrow; low levels of HoxB7/Cre activity were also detected in the dorsal root ganglia (arrowhead) and the spinal cord). (C) The ureteric bud has branched once in the metanephric mesenchyme (arrow). (D) The ureteric bud has undergone several branches, the ureter (arrow) and the Wolffian duct (arrowhead) are evident. (E,F) Sections of different regions of a E12.5 kidney. (G-I) The β-galactosidase activity was high in ureteric bud derivatives of the Z/AP kidney in the absence of *HoxB7/Cre* (G), but was completely removed in the presence of *HoxB7/Cre* (H). Alkaline phosphatase activity was detected in all ureteric bud branches (I).

Shh signaling is required for mesenchymal cell proliferation

The mutant kidneys in newborn pups were 52% smaller than those in their wild-type littermates (Fig. 5A; wild type, n=3; mutant, n=4; P=0.002), and the glomerular number was reduced by 40% (P=0.004). However, the glomerular density in the mutant kidneys increased by 26% (Fig. 4B, P=0.03). To determine if this increase in glomerular density is due to differential effects of *Shh* on cortical and medullary regions of the kidney (*Shh* expression is primarily in the medulla), we further quantified the cortical and medullary volume. The reduction of the cortical and the medullary volume of *Shh* mutants is similar, 51% (P=0.003) and 46% (P=0.002), respectively. The cortical glomerular density in mutant kidneys increased by 24% (P=0.02), similar to that of the whole mutant kidneys. These data suggest that the higher glomerular density in the entire mutant kidney is not due to the underdevelopment of the medullary region relative to the rest of the kidney. No gross size differences were seen between the glomerulus of the mutant kidneys and that of the wild type.

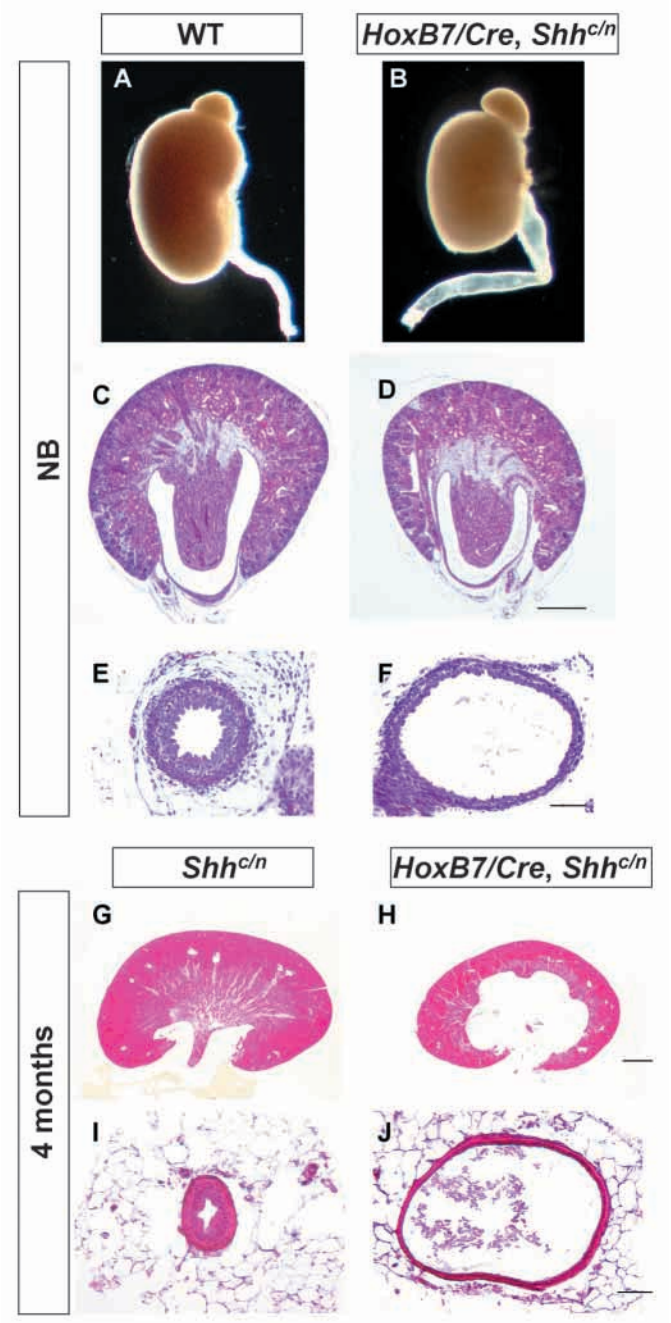

Fig. 3. Conditional removal of *Shh* activity from the urothelium with HoxB7/Cre results in hypoplasia, hydroureter and hydronephrosis. (A,B) Whole-mount view of the newborn kidney and ureter of wild-type (WT) and *HoxB7/Cre, Shh$^{c/n}$* mice. (C-J) Hematoxylin and Eosin staining of coronal sections (C,D) and parasagittal sections (G,H) of the kidney (C,D,G,H) and cross-sections of the ureter (E,F,I,J) at stages indicated. Scale bars: 500 μm in C,D; 100 μm in E,F,I,J; 1 mm in G,H.

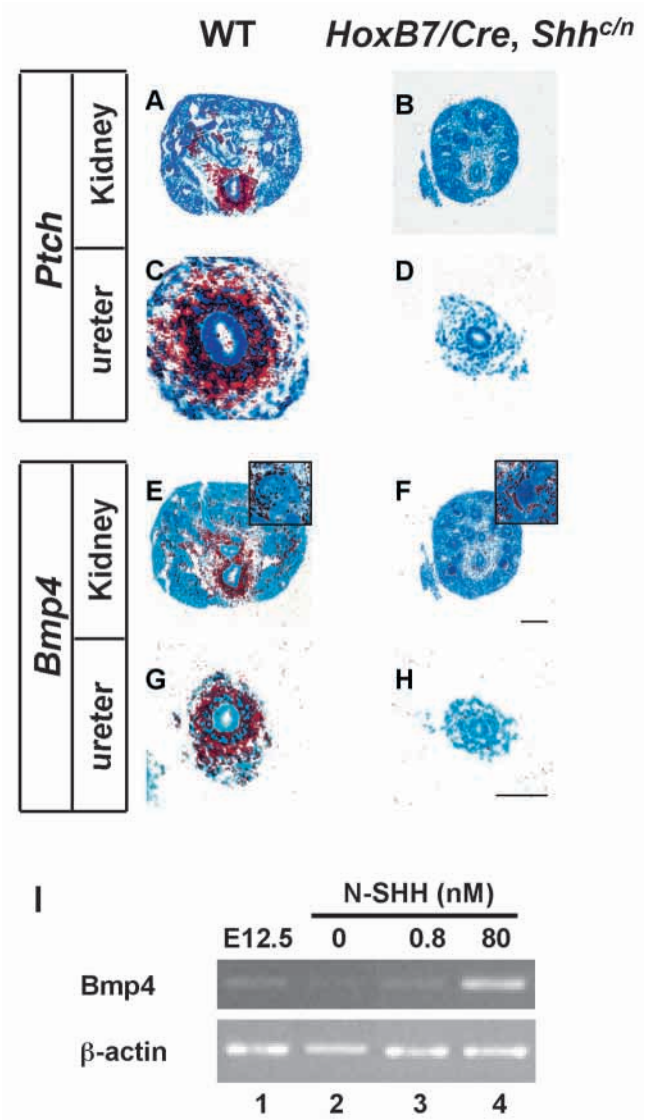

Fig. 4. *Ptch* and *Bmp4* expression in mutant kidneys. (A-H) In situ hybridization of *Ptch* and *Bmp4* probes to E14.5 kidney (A,B,E,F) and ureter (C,D,G,H). The insets show *Bmp4* expression in glomeruli. Scale bars: 100 μm in A,B,E,F; 50 μm in C,D,G,H. (I) RT-PCR of *Bmp4* transcripts from E12.5 mesenchymal cells dissected from the ureter (lane 1) and those cultured without (lane 2) and with (lanes 3 and 4) the addition of N-SHH protein at concentrations indicated. PCR with β-actin primers (β-actin) indicated equal cDNA inputs in all lanes.

Consistent with the hypoplasia in the kidney, the length of the E14.5 mutant ureter was about 21% shorter than that of the wild-type littermates (n=5, P=0.03), and fewer mesenchymal cells lined the ureteral epithelium of mutants (data not shown). Taken together, these data suggest that *Shh* is involved in survival and/or proliferation of mesenchymal cells in the kidney and ureter.

Ptch expression indicates that mesenchymal cells adjacent to the *Shh* expression domain are the target of *Shh* signaling. We therefore focused our analysis on these cells, in particular, the condensed mesenchymal cells surrounding the epithelium of the ureter that are a morphologically distinct population of cells that respond strongly to Shh signaling at E14.5 (cells within the dotted circle, Fig. 5C,D). We examined the effect of removal of Shh signaling on cell proliferation and apoptosis in this cell population. Ureter sections were immunostained for phospho-histone H3, in order to quantify cells in M phase of the cell cycle and thereby measure the mitotic index (Fig. 5C-E). In the proximal ureter of the mutants, the mitotic index of cells in the subjacent mesenchyme that normally demarcates the *Shh*-responsive zone was 52% that of wild-type littermates (Fig. 5E proximal, n=4, P=0.004). In the distal ureter, the mitotic index of this population of cells was 48% that of the wild-type littermates (Fig. 5E distal, P=0.05). Thus, cell proliferation is greatly reduced in *Shh* mutants. TUNEL analysis of the ureteral mesenchyme detected no significant difference in cell death between mutant and wild-type tissues (data not shown), indicating that apoptosis was unlikely to play a role in the generation of the mutant phenotype.

We further examined the role of *Shh* in cell proliferation with primary ureteral mesenchymal cell cultures. Mesenchymal cells dissected from E12.5 ureter were cultured in the absence of serum. Each culture was supplemented with 50 ng/ml FGF-2 and 10 ng/ml TGF-α to maintain ureteral mesenchymal cells which rapidly die in the absence of these factors (SHH alone did not support ureteral mesenchymal cell survival in the culture without these factors; J. Y. and A. P. M., unpublished). Approximately 4.8% of cells cultured in FGF-2 and TGF-α alone (control) were actually proliferating (in S phase), while this number significantly increased to 14.0% of mesenchymal cells cultured with 0.8 nM N-SHH protein (SHH; Fig. 5F, P=0.007). The observation that *Shh* can promote ureteral mesenchymal cell proliferation in vitro correlates well with the reduction of proliferation of this *Shh*-responsive cell population in *Shh* mutant kidneys.

Bmp4 expression has been shown to be regulated by Shh signaling in several tissues and its *Drosophila* counterpart *Dpp* is a target of *Drosophila* Hedgehog (for reviews, see Ingham and McMahon, 2001; McMahon et al., 2002). *Bmp4* was co-expressed with *Ptch* in mesenchymal cells surrounding the *Shh*-expressing collecting ducts (Fig. 4E) and the ureter (Fig.

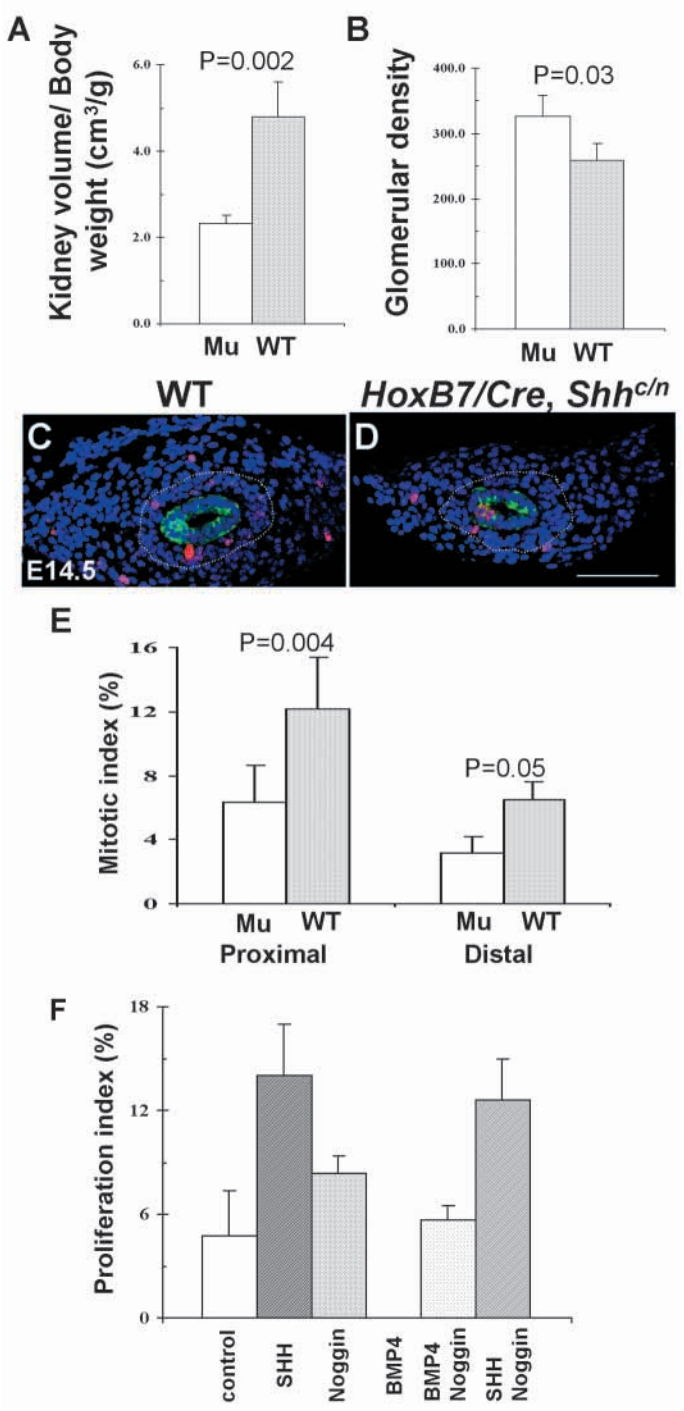

Fig. 5. *Shh* is required for mesenchymal cell proliferation. (A) The kidney volume/body weight of *Shh* mutant (Mu, n=4; 2.3±0.2 cm^3/g) and wild-type (WT, n=3; 4.8±0.8 cm^3/g) kidneys at the newborn stage. (B) The glomerular density of *Shh* mutant (Mu, 326.32±33.07) and wild-type (WT, 258.89±25.77) kidneys at the newborn stage. (C-E) Ureter sections from E14.5 wild-type (C) or mutant (D) kidneys were stained with anti-phospho-histone H3 antibodies (red), *Dolichos bifloris* agglutinin, which demarcates the surface of the epithelium (DBA, green), and a DNA dye (DAPI; blue). Mesenchymal cells within the broken line were counted for calculations in E. The mitotic index of the proximal ureter mesenchyme was 6.29±2.39% in *Shh* mutants (Mu) and 12.12±3.24% in wild-type (WT). The mitotic index of the distal ureter mesenchyme was 3.15±1.05% in *Shh* mutants and 6.5±1.08% in wild type. Scale bar: 50 μm in C,D. (F) Mesenchyme dissected from E12.5 ureter was cultured for 5 days without (control) or with proteins as indicated (see Materials and Methods), labeled with 10 μM BrdU for 11 hours and stained with anti-BrdU antibodies and the DNA dye DAPI. Proliferation index was calculated as the percentage of nuclei that incorporated BrdU. Control, 4.8%; SHH, 14.0%; Noggin, 8.4%; BMP4, 0%; BMP4+Noggin, 5.7%; SHH+Noggin, 12.6%.

4G) in wild-type embryos. *Bmp4* expression in this domain was abolished in *Shh* mutant kidneys at E14.5, indicating that *Bmp4* expression depended on Shh signaling (Fig. 4F,H). As expected, expression of *Bmp4* in glomeruli was not affected in *Shh* mutants (Fig. 4F, inset).

To further test the dependence of *Bmp4* expression on *Shh* signaling in ureteral mesenchyme, we examined *Bmp4* expression in cultured ureteral mesenchymal cells in the presence or absence of N-SHH protein (Fig. 4I). *Bmp4* levels increased on addition of N-SHH protein, lending support to the conclusion that *Bmp4* is a potential target of Shh signaling to the ureteral mesenchyme. Furthermore, the levels of *Bmp4* expression observed in cultures in the absence of N-SHH (Fig. 5I, lane2) were lower than freshly dissected ureteral mesenchyme (Fig. 5I, lane1) is consistent with Shh-mediating maintenance of *Bmp4* expression.

The fact that *Bmp4* appears to be downstream of Shh signaling raised the possibility that the proliferative function of *Shh* is mediated through *Bmp4*. However, when ureteral mesenchyme was cultured with 0.8 nM N-SHH and the potent BMP4 antagonist, 300 ng/ml noggin, to block Bmp4 signaling, there was no significant difference in the stimulation of proliferation than that observed in cells cultured with N-SHH alone (Fig. 5F). Furthermore, addition of 100 ng/ml BMP4 completely blocked proliferation, indicating that BMP4 is anti-mitogenic for this cell population (Fig. 5F). The anti-proliferative effects of BMP4 were antagonized by addition of 300 ng/ml Noggin, the same concentration used in the SHH/Noggin co-culture experiment, demonstrating that Noggin was active in these assays (Fig. 5F). Noggin alone had no statistically significant proliferative effect on the cultures (Fig. 5F; noggin, P=0.12). Taken together, these results suggest that the proliferative function of Shh was not mediated by *Bmp4*, supporting a more direct action of Shh signaling. Furthermore, that Shh stimulated cell proliferation while at the same time inducing *Bmp4* expression suggests that *Shh* can overcome the inhibitory effect of *Bmp4*.

Smooth muscle differentiation in the ureteral mesenchyme is delayed in *Shh* mutant kidneys

Smooth muscle forms from condensed mesenchyme that underlies the urothelium in the ureter and the renal pelvis (McHugh, 1995). The peristaltic movement of smooth muscles propels urine from the renal pelvis to the bladder and relieves the kidney paranchyma from the damaging pressure that fluid build-up causes. *Bmp4* has been shown to promote formation of smooth muscle in the kidney and ureter (Raatikainen-Ahokas et al., 2000). The hydroureter phenotype and the expression pattern of *Shh* and *Ptch* in the ureter and the renal pelvis along with the lack of *Bmp4* expression prompted us to examine smooth muscle formation in the mutant kidneys.

The timing and pattern of smooth muscle differentiation in the mouse kidney and ureter was not well documented. Initially, we characterized normal smooth muscle differentiation in wild-type kidneys. At E13.5, mesenchymal cells condense around the epithelium. However, the absence of smooth muscle α-actin protein (SMA), an early marker of smooth muscle differentiation, indicated that smooth muscle differentiation had not occurred (data not shown). At E14.5, SMA was detected in scattered condensed mesenchymal cells of the proximal ureter (closer to the kidney, Fig. 6A,B, arrow)

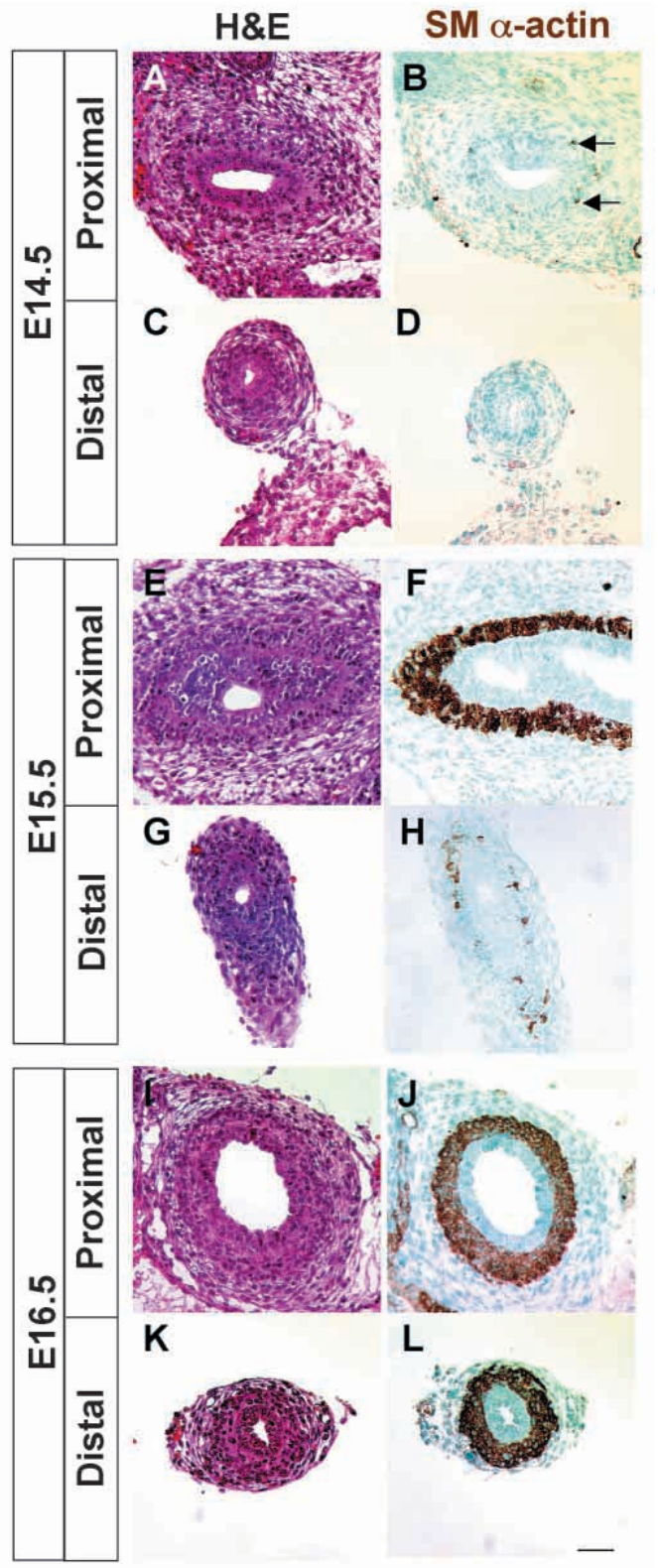

Fig. 6. Smooth muscle differentiation in wild-type kidneys and ureter. Hematoxylin and Eosin (H&E; A,C,E,G,I,K) and immunohistochemical staining for smooth muscle α-actin (SM α-actin, brown; B,D,F,H,J,L) in the proximal (A,B,E,F,I,J) and distal (C,D,G,H,K,L) ureter at the indicated stages. Arrows in B indicate scattered cells that produce SM α-actin. Scale bar: 50 μm.

and the future renal pelvis (data not shown), but not the distal ureter (closer to the bladder, Fig. 6C,D). At E15.5, distal ureteral mesenchymal cells started to produce SMA (Fig. 6G,H), while the majority of condensed mesenchymal cells in the proximal ureter (Fig. 6E,F) and the future pelvis (data not shown) show abundant SMA protein. By E16.5, SMA was present along the entire length of the ureter (Fig. 6I-L) and the renal pelvis (data not shown). Unlike the situation in the rat (Baker and Gomez, 1998), but similar to that in humans (Tacciuoli et al., 1975; Matsuno et al., 1984), smooth muscle differentiation in the mouse ureter forms in a descending direction (from the kidney to the bladder) along the proximodistal axis of the ureter.

In *Shh* mutant kidneys at E15.0, no SMA was detected at any axial level of the ureter in contrast to wild-type embryos where SMA production was detected in the proximal ureter (Fig. 7A-D). At the newborn stage, SMA was detected in the proximal ureter of *Shh* mutants (Fig. 7E,F), but in contrast to wild-type littermates, the number of mesenchymal cells that produced SMA decreased in more distal regions such that almost no SMA was detected in the distal-most part of the ureter, closest to the bladder (Fig. 7G,H). Furthermore, mesenchymal cells in the distal ureter were not as condensed as those of wild-type siblings. Histological examination at the newborn stage indicates that SMA-positive cells in wild-type and mutants are smooth muscle cells. Taken together, these data indicate that some smooth muscle formation occurs in *Shh* mutant kidneys, but formation was delayed and the number of SMA-producing cells was greatly reduced at birth. The decrease in the number of SMA-producing cells from proximal to distal end of the ureter in mutants is in good agreement with the sequence of smooth muscle differentiation in the wild type, reflecting a general delay in smooth muscle differentiation along the length of the ureter. That some smooth muscle differentiation occurred in the *HoxB7/Cre*, *Shh*$^{c/n}$ mutants is not due to the ineffective removal of *Shh* activity by the *Cre*-mediated recombination, as ureteral mesenchyme from kidneys of *Shh* null mice also produced SMA (data not shown).

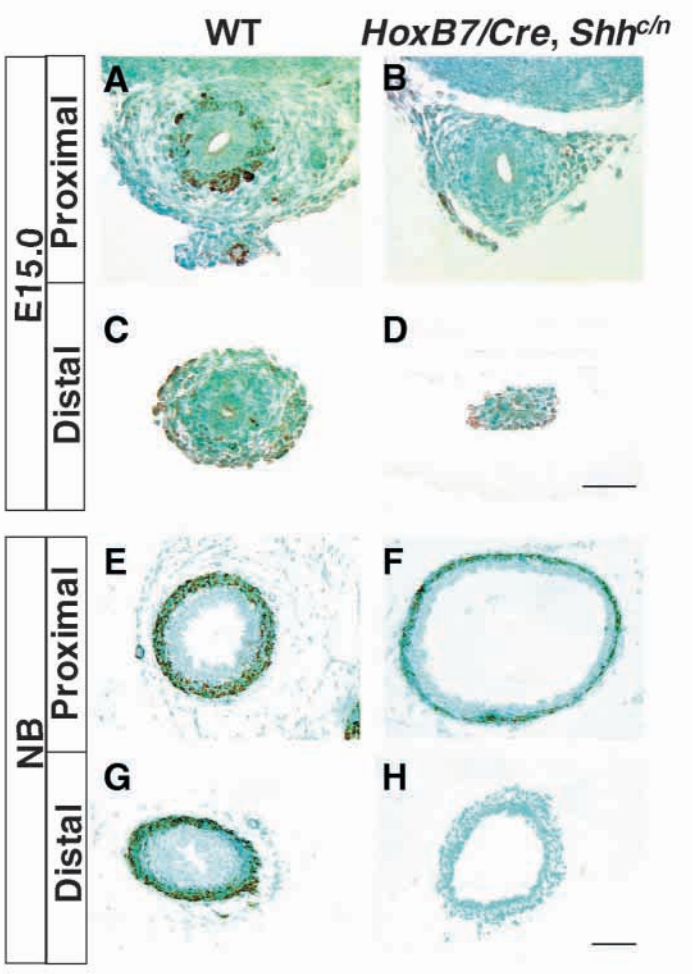

Fig. 7. Smooth muscle differentiation in the wild-type (A,C,E,G) and *Shh* mutant (B,D,F,H) kidneys. Immunohistochemical staining for smooth muscle α-actin (brown) in the cross-sections of the proximal (A,B,E,F) and distal (C,D,G,H) ureters at the stages indicated. NB, newborn. Scale bar: 50 μm in A-D; 100 μm in E-H.

Shh inhibits smooth muscle formation in a dose-dependent manner

Smooth muscle formation in the ureter has been reported to occur in cells immediately adjacent to the urothelium, a similar position to smooth muscle in the respiratory system (McHugh, 1995), which is also Shh dependent (Pepicelli et al., 1998). Close observation of newborn ureters detected 1-2 layers of ureteral mesenchymal cells that are SMA negative between the SMA-positive smooth muscle and the ureteral epithelium (arrow, Fig. 8A). We refer to these cells as the subepithelial ureteral mesenchymal cells for simplicity. No such cells are detected in the renal pelvis (data not shown). In the proximal ureter of *Shh* mutants, this cell population was completely absent (Fig. 8B), suggesting that these cells required Shh signaling for their establishment and/or maintenance.

To determine if the sub-epithelial ureteral mesenchymal cells were directly *Shh* responsive, we examined ureters from *Ptch-lacZ*$^{+/-}$ newborn mice in which *lacZ* was knocked into the *Ptch* locus (Goodrich et al., 1997). X-gal staining of these mice faithfully recapitulated the endogenous *Ptch* expression pattern in many tissues including the kidney and ureter (Goodrich et al., 1997) (Fig. 8C and data not shown). The β-gal-positive cells in the ureter were SMA negative and lay directly adjacent to the epithelium (Fig. 8D, arrow). Therefore, the subepithelial ureteral mesenchymal cells appear to be the subset of ureteral mesenchymal cells that respond to high-level Shh signaling at the newborn stage. As *Ptch* was expressed in all the likely smooth muscle progenitor cells that appear as condensed mesenchyme around the ureteral epithelium before the initiation of SMA production at E14.5 (Fig. 1C), but not in SMA-producing cells later in development, it would appear that smooth muscle progenitor cells, but not differentiated smooth muscle cells, normally respond to Shh signaling. The subepithelial ureteral mesenchymal cells, closest to the Shh signaling source, responded to *Shh* signaling but did not produce SMA, suggesting that high levels of Shh signaling may in fact inhibit smooth muscle differentiation. To address this issue, we assayed smooth muscle α-actin expression in ureteral mesenchymal cultures in response to N-SHH (Fig. 8E). Smooth muscle α-actin expression could be detected by RT-PCR as early as E12.5 in the ureteral mesenchyme (Fig. 8E, lane 1), and cells cultured for 5 days without N-SHH protein still expressed smooth muscle α-actin (Fig. 8E, lane 2).

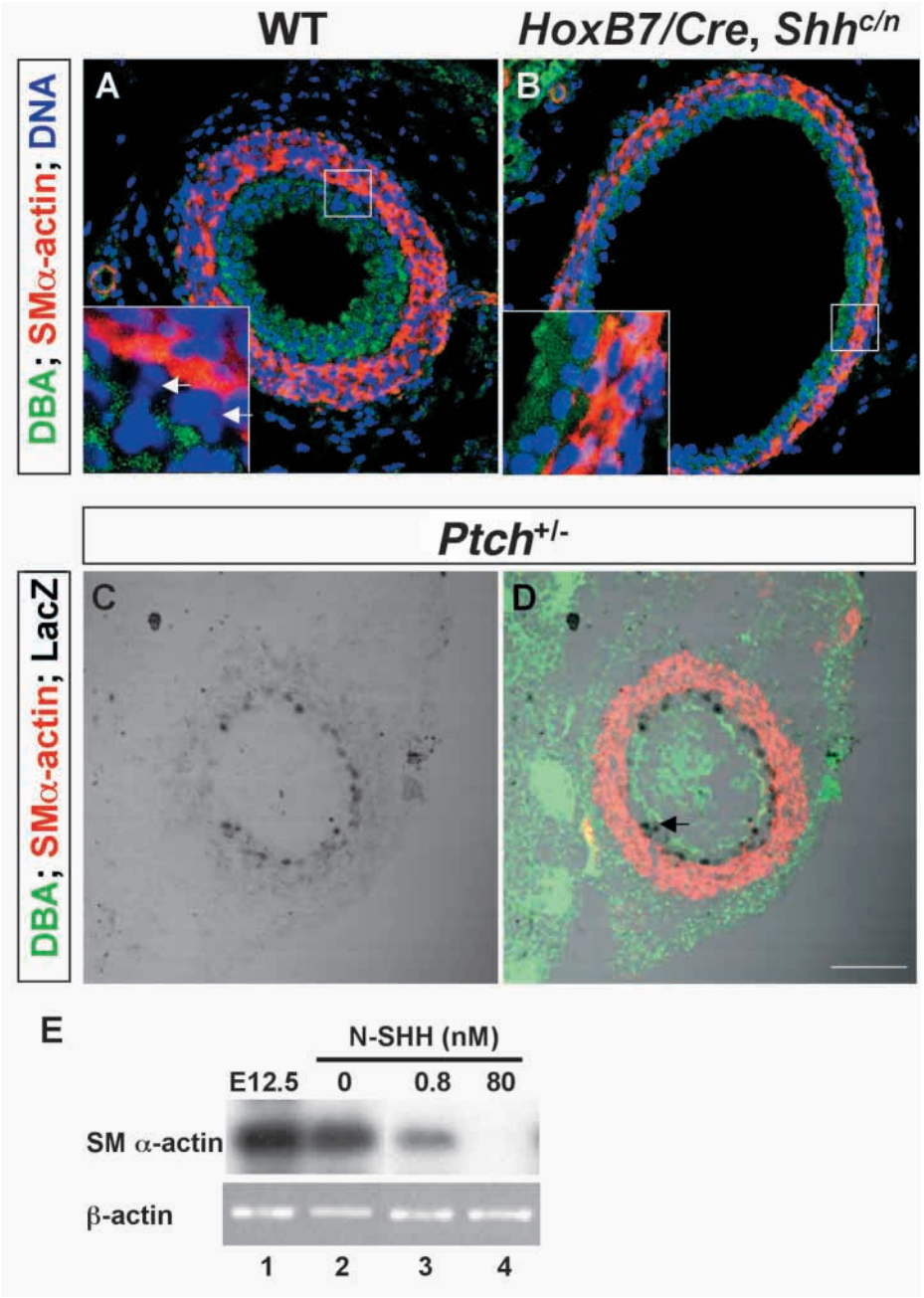

Fig. 8. Mesenchymal cells between smooth muscle and the epithelium in the ureter are absent in *Shh* mutants. (A,B) Newborn kidneys and ureters stained with anti-smooth muscle α-actin antibody (red), *Dolichos bifloris* agglutinin (DBA), which stains the cell surface and demarcates the urothelium (green), and the DNA dye DAPI (blue). Note that one to two layers of mesenchymal cell nuclei immediately subjacent to the ureteral epithelium (the boundary marked by DBA staining) in the ureter of wild type are not surrounded by anti-smooth muscle α-actin antibody staining (A; inset, arrow), suggesting that these cells do not express smooth muscle α-actin. By contrast, in the mutants (B; inset), those cells recognized by the anti-smooth muscle α-actin antibody lie immediately adjacent to the urothelium (the boundary marked by DBA staining). Thus, the smooth muscle α-actin-negative mesenchymal cell population appears to be absent in *HoxB7/Cre*, $Shh^{c/n}$ kidneys. (C,D) *Ptch-lacZ*$^{+/-}$ mice at the newborn stage stained for β-galactosidase (black), smooth muscle α-actin (red) and *Dolichos bifloris* agglutinin (DBA, green) indicates that those cells expressing highest level of *Ptch-lacZ* do not produce SMA. Arrow in D indicates such cells. Scale bar: 50μm. (E) *Shh* adversely affects smooth muscle differentiation in a dose-dependent manner. RT-PCR of *SM α-actin* (SM α-actin) transcripts from E12.5 mesenchymal cells dissected from the ureter (lane 1) and those cultured without (lane 2) and with (lanes 3 and 4) the addition of N-SHH protein at concentrations indicated. PCR with β-actin primers (β-actin) indicated equal cDNA inputs in all lanes.

However, addition of 0.8 nM N-SHH greatly reduced, and addition of 80 nM N-SHH completely abolished, the expression of smooth muscle α-actin (Fig. 8E, lanes 3 and 4). Thus, *Shh* inhibits smooth muscle differentiation in ureteral mesenchyme cultures in a dose-dependent fashion.

DISCUSSION

The developmental function of the distal collecting duct and ureteral epithelium is largely unknown. In this study, we examined the role of *Shh*, a signaling molecule expressed in these regions during metanephric kidney development. We showed that Shh signaling acts on mesenchymal cells underlying the urothelium, to regulate their proliferation and the timing and pattern of their differentiation. These results may have significant implications for the etiology of renal anomalies associated with deletions of the Shh-encoding region of chromosome 7q36 in humans.

Shh and mesenchymal cell proliferation

Collectively our analyses of *Shh* mutants and the response of ureteral mesenchyme in vitro indicated that Shh served as a mitogen to promote proliferation of ureteral mesenchymal cells. This effect is likely to extend to the mesenchyme in the kidney proper, which abutted the *Shh*-expressing collecting duct epithelium and had elevated level of *Ptch* expression. The decreased proliferation of medullary mesenchyme is likely to play a major role in the observed hypoplasia of *Shh* mutant kidneys. The proliferative effect of *Shh* was not mediated by

its downstream target gene, *Bmp4*, but was probably direct, as *Ptch* expression was upregulated in the proliferative zone. Other proliferative factors, such as *Fgf7*, have been reported to play a role in proliferation of kidney tissues (Qiao et al., 1999). However, *Fgf7* acts primarily on the collecting duct epithelium, and it is therefore unlikely to mediate Shh-directed stimulation of mesenchymal cell proliferation. *Shh* has been shown to play important roles in regulating cell proliferation in many tissues, such as the gut mesencyme, the early hair follicles and the central nervous system (for reviews, see Ingham and McMahon, 2001; McMahon et al., 2002). The finding that *Shh* stimulates cell proliferation in kidney formation adds to the evidence for a mitogenic action of *Shh* in developing target tissues, a role shared by *Ihh*, which has a mitogenic function in the developing endochondral skeleton (Long et al., 2001; St-Jacques et al., 1999).

Shh and kidney smooth muscle differentiation

The mesenchymal cells in the ureter adopt two fates, correlating with their position relative to the ureteral epithelium. The subepithelial ureteral mesenchymal cells, which are closest to the Shh source and presumably receive the highest level of Shh activity, do not differentiate into smooth muscle at least by the newborn stage, smooth muscle differentiation is restricted to cells further away from the epithelium.

The role of *Shh* in differentiation of smooth muscle progenitor cells into smooth muscle in the ureter is complicated. Although we see that smooth muscle forms in the absence of Shh signaling in vivo, as expected from the in vitro data, smooth muscle differentiation is delayed. How can an inhibitor of smooth muscle differentiation apparently also promote smooth muscle formation? One possibility is that this promotion is a secondary effect from the proliferative effect of *Shh* on smooth muscle progenitor cells (Fig. 9). It is possible that only when these progenitor cells proliferate to reach a certain cell number/density will smooth muscle differentiation initiate. For example, a specific cell mass may be required to establish sufficient levels of a smooth muscle differentiation signal. Consequently, a reduced proliferation rate in *Shh* mutants would be expected to reduce the production of such a differentiation signal and delay smooth muscle differentiation even if the inhibitory effect of *Shh* on smooth muscle differentiation is removed. A similar observation has been made in *Ihh* mutants, where delay in chondrocyte proliferation appears to retard the initiation of chondrocyte differentiation even though *Ihh* normally inhibits the differentiation process (Karp et al., 2000; Long et al., 2001; St-Jacques et al., 1999).

Shh may also promote smooth muscle formation in vivo through its induction of some smooth muscle differentiation factors. *Bmp4* is a vertebrate homolog of *Drosophila Decapentaplegic*, which is a downstream target gene of Hh signaling in the fly. In mouse, *Bmp4* is expressed adjacent to *Shh* expressing cells in many tissue types (Bitgood and McMahon, 1995). There is also some evidence that *Bmp4* may also be a downstream target of *Shh* (for reviews, see Ingham and McMahon, 2001; McMahon et al., 2002). In this study, we show that *Bmp4* expression is positively regulated by *Shh* signaling in renal mesenchyme. *Bmp4* has been shown to promote smooth muscle differentiation in the ureter (Raatikainen-Ahokas et al., 2000). It is likely that one way *Shh*

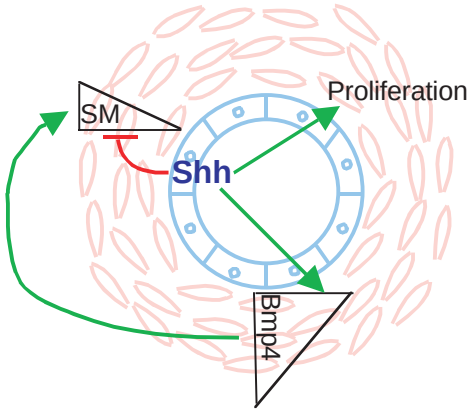

Fig. 9. A model for the functions of Shh in ureteral mesenchymal cell proliferation and differentiation. Shh produced in the ureteral epithelium promotes proliferation and inhibits smooth muscle differentiation of ureteral mesenchymal cells. It also induces *Bmp4* expression in these cells. SM, smooth muscle.

promotes smooth muscle differentiation in smooth muscle progenitor cells is through its induction of smooth muscle differentiation factors such as *Bmp4* in these cells, although the fact that smooth muscle formation still occurs in the absence of *Shh* and *Bmp4* suggests that *Bmp4* is not essential for renal smooth muscle formation. One can imagine several possibilities to explain these results. For example, smooth muscle progenitor cells may also receive (and produce) other smooth muscle differentiation factors, the production of which is independent of Shh signaling.

The loss of the subepithelial ureteral mesenchymal cells in *Shh* mutants suggests that Shh signaling is required for establishment and/or maintenance of this population. Our in vitro data further showed that *Shh* inhibits smooth muscle formation in the ureteral smooth muscle progenitor cells in a dose-dependent manner. Together, these data are consistent with a model in which *Shh* establishes and/or maintains these subepithelial ureteral mesenchymal cells by active inhibition of their differentiation (Fig. 9). The simplest scenario is that in the absence of *Shh* signaling, these cells differentiate into smooth muscle. However, to prove this is the case would require a scheme whereby the fate of these cells could be tracked in vivo: this is, unfortunately, beyond our current capabilities.

By contrast, within the renal pelvis at the newborn stage, we do not detect a population of SMA-negative cells in the equivalent region, even though the subjacent mesenchymal cells also express *Ptch*, which is indicative of Shh signaling. One possible explanation of this regional difference could be that the actual levels of Shh signaling might be insufficient in the renal pelvis to inhibit all cells from adopting a smooth muscle fate.

The subepithelial ureteral mesenchymal cells receive the highest level of *Bmp4* and probably other smooth muscle differentiation factors. How can *Shh* inhibit their response to these differentiation factors? It is possible that the high levels of *Shh* that these cells receive blocks their ability to respond to smooth muscle differentiation factors they themselves and their neighbor cells produce. In the *Drosophila* wing imaginal disc, Hh represses the expression of the *Dpp* receptor in cells in the anterior compartment immediately neighboring the Hh-

expressing cells, thus blocking their response to the high level of *Dpp* they produce, whereas cells farther away from *Hh* sources express *Dpp* in response to Hh and also respond to *Dpp* (Tanimoto et al., 2000). A similar mechanism could exist in the ureter. Alternatively, *Shh* may induce the expression of antagonists to these differentiation factors in these cells. Unfortunately, we cannot examine these possibilities now because of the lack of knowledge of all the smooth muscle differentiation factors that are involved in kidney development. However we have ruled out the possible roles of two of Bmp4 antagonists, noggin and gremlin, in this process, as their expression was not detected in the kidney and ureter at E14.5, the time when smooth muscle differentiation initiates and therefore inhibition of smooth muscle formation in the subepithelial ureteral mesenchymal cells should be active (J. Y. and A. P. M., unpublished).

The opposing effects of the promotion of proliferation of smooth muscle progenitor cells by *Shh* together with the induction of a smooth muscle differentiation signal, and the inhibitory effect of *Shh* on smooth muscle differentiation may serve to ensure correct timing and pattern of smooth muscle differentiation (Fig. 9). Our finding that *Shh* inhibits smooth muscle formation in the kidney is in line with studies carried out in chick gut (Sukegawa et al., 2000), where it appears that gut epithelium-derived *Shh* inhibits smooth muscle formation in mesenchymal cells closest to the epithelium, regulating the radial pattern of mesenchymal differentiation. However, in that case, the effect of *Shh* on the timing of smooth muscle differentiation in the mesenchyme further away from the epithelium was not examined. It is tempting to speculate that the role of *Shh* in visceral smooth muscle formation is conserved in different organs.

Shh and hydroureter

One of the most obvious defects in *Shh* mutant kidneys is hydroureter/hydronephrosis. Hydronephrosis is likely to be a secondary consequence of hydroureter, as hydroureter was apparent first and the back pressure produced from hydroureter is thought to trigger hydronephrosis. Malformation and destruction of various urinary tract structures are associated with hydroureter. As the dilation of the ureter was usually more severe or only detected in the proximal ureter of *Shh* mutant kidneys, the defect is unlikely to result from a UVJ (ureterovesical junction) abnormality, which would be expected to result in a dilation of the distal ureter. Furthermore, we always detected a lumen along the entire length of the *Shh* mutant ureter, with no evidence of a ureteral valve (a reduplication of the transitional epithelium folds that protrude into the lumen), thus ruling out a possible anatomical obstruction. It is difficult to speculate how the lack of the subepithelial ureteral mesenchymal cells may contribute to hydroureter, before the fate of this cell population is identified. These cells may give rise to smooth muscle cells, or they may generate other cell types such as the lamina propria, a layer of connective tissue between the urothelium and smooth muscle.

Whatever the exact fate of these subepithelial ureteral mesenchymal cells is, the reduction of smooth muscle in the ureter is likely to play a causal role in the observed hydroureter. Smooth muscle functions to propel urine from the renal pelvis to the bladder. The reduced amount of smooth muscle in the ureter of *Shh* mutant kidneys is likely to compromise the transport of urine to the bladder, hence to cause the build-up of urine in the ureter. The observed more dilated proximal ureter where fluid builds up is consistent with smooth muscle formation in the distal ureter being more severely affected. Malformation of smooth muscle is also associated with congenital ureteral stricture in humans, which leads to hydroureter/hydronephrosis (Culp, 1981; Tanagho, 1981). Interestingly, hydroureter has been reported in some cases of human infants with a chromosomal deletion of a *Shh*-encoding region (Lurie et al., 1990; Nowaczyk et al., 2000), suggesting that a deficiency in SHH might lead to a similar phenotype in the human kidney. The mouse *Shh* mutant kidney may therefore serve as an animal model system for understanding the ontogeny of smooth muscle formation, the pathogenesis of human congenital ureteral stricture, the hydroureter associated with a deficiency in Shh signaling and for the possible development of treatments for these defects in humans.

We thank Nancy Wu for transgenic construct injection; Diane Faria and Bianca Klumpar for histology; Dr J. Deschamps for the HoxB7 promotor/enhancer fragment; and Drs Arindam Majumdar, M. Todd Valerius, George Yip and Paula M. Lewis for critical comments. This work was supported by a Research Fellowship from the National Kidney Foundation to J. Y., ACS grant PF00010001DDC to T. J. C. and NIH grant DK54364 to A. P. M.

REFERENCES

Aufderheide, E., Chiquet-Ehrismann, R. and Ekblom, P. (1987). Epithelial-mesenchymal interactions in the developing kidney lead to expression of tenascin in the mesenchyme. *J. Cell Biol.* **105**, 599-608.

Baker, L. A. and Gomez, R. A. (1998). Embryonic development of the ureter and bladder: acquisition of smooth muscle. *J. Urol.* **160**, 545-550.

Bertram, J. F., Soosaipillai, M. C., Ricardo, S. D. and Ryan, G. B. (1992). Total numbers of glomeruli and individual glomerular cell types in the normal rat kidney. *Cell Tissue Res.* **270**, 37-45.

Bitgood, M. J. and McMahon, A. P. (1995). Hedgehog and Bmp genes are coexpressed at many diverse sites of cell-cell interaction in the mouse embryo. *Dev. Biol.* **172**, 126-138.

Chaffin, K. E., Beals, C. R., Wilkie, T. M., Forbush, K. A., Simon, M. I. and Perlmutter, R. M. (1990). Dissection of thymocyte signaling pathways by in vivo expression of pertussis toxin ADP-ribosyltransferase. *EMBO J.* **9**, 3821-3829.

Culp, D. A. (1981). Congenital anomalies of the ureter. In *The Ureter* (ed. H. Bergman), pp. 625-646. New York: Springer-Verlag.

Dassule, H. R., Lewis, P., Bei, M., Maas, R. and McMahon, A. P. (2000). Sonic hedgehog regulates growth and morphogenesis of the tooth. *Development* **127**, 4775-4785.

Dudley, A. T. and Robertson, E. J. (1997). Overlapping expression domains of bone morphogenetic protein family members potentially account for limited tissue defects in BMP7 deficient embryos. *Dev. Dyn.* **208**, 349-362.

Ekblom, P. (1992). *Renal Development*. New York: Raven.

Erickson, R. A. (1968). Inductive interactions in the development of the mouse metanephros. *J. Exp. Zool.* **169**, 33-42.

Gillenwater, J. Y. (1992). *The Pathophysiology of Urinary Tract Obstruction*. Philadelphia: WB Saunders.

Goodrich, L. V., Milenkovic, L., Higgins, K. M. and Scott, M. P. (1997). Altered neural cell fates and medulloblastoma in mouse patched mutants. *Science* **277**, 1109-1113.

Grobstein, C. (1953). Inductive epithelio-mesenchymal ineraction in cultured organ rudiments of the mouse. *Science* **118**, 52-55.

Grobstein, C. (1955). Inductive interraction in the development of the mouse metanephros. *J. Exp. Zool.* **130**, 319-339.

Herzlinger, D., Koseki, C., Mikawa, T. and al-Awqati, Q. (1992). Metanephric mesenchyme contains multipotent stem cells whose fate is restricted after induction. *Development* **114**, 565-572.

Ingham, P. W. and McMahon, A. P. (2001). Hedgehog signaling in animal development: paradigms and principles. *Genes Dev.* **15**, 3059-3087.

Karavanova, I. D., Dove, L. F., Resau, J. H. and Perantoni, A. O. (1996). Conditioned medium from a rat ureteric bud cell line in combination with bFGF induces complete differentiation of isolated metanephric mesenchyme. *Development* **122**, 4159-4167.

Karp, S. J., Schipani, E., St-Jacques, B., Hunzelman, J., Kronenberg, H. and McMahon, A. P. (2000). Indian hedgehog coordinates endochondral bone growth and morphogenesis via parathyroid hormone related-protein-dependent and -independent pathways. *Development* **127**, 543-548.

Kim, P. C., Mo, R. and Hui, C. C. (2001). Murine models of VACTERL syndrome: Role of sonic hedgehog signaling pathway. *J. Pediatr. Surg.* **36**, 381-384.

Kress, C., Vogels, R., de Graaff, W., Bonnerot, C., Meijlink, F., Nicolas, J. F. and Deschamps, J. (1990). Hox-2.3 upstream sequences mediate lacZ expression in intermediate mesoderm derivatives of transgenic mice. *Development* **109**, 775-786.

Lewis, P. M., Dunn, M. P., McMahon, J. A., Logan, M., Martin, J. F., St-Jacques, B. and McMahon, A. P. (2001). Cholesterol modification of sonic hedgehog is required for long-range signaling activity and effective modulation of signaling by Ptc1. *Cell* **105**, 599-612.

Lobe, C. G., Koop, K. E., Kreppner, W., Lomeli, H., Gertsenstein, M. and Nagy, A. (1999). Z/AP, a double reporter for cre-mediated recombination. *Dev. Biol.* **208**, 281-292.

Long, F., Zhang, X. M., Karp, S., Yang, Y. and McMahon, A. P. (2001). Genetic manipulation of hedgehog signaling in the endochondral skeleton reveals a direct role in the regulation of chondrocyte proliferation. *Development* **128**, 5099-5108.

Lurie, I. W., Ilyina, H. G., Podleschuk, L. V., Gorelik, L. B. and Zaletajev, D. V. (1990). Chromosome 7 abnormalities in parents of children with holoprosencephaly and hydronephrosis. *Am. J. Med. Genet.* **35**, 286-288.

Matsuno, T., Tokunaka, S. and Koyanagi, T. (1984). Muscular development in the urinary tract. *J. Urol.* **132**, 148-152.

McHugh, K. M. (1995). Molecular analysis of smooth muscle development in the mouse. *Dev. Dyn.* **204**, 278-290.

McMahon, A. P., Ingham, P. W. and Tabin, C. (2002). The developmental roles and clinical significance of Hedgehog signaling. *Curr. Top. Dev. Biol.* (in press).

Miyazaki, Y., Oshima, K., Fogo, A., Hogan, B. L. and Ichikawa, I. (2000). Bone morphogenetic protein 4 regulates the budding site and elongation of the mouse ureter. *J. Clin. Invest.* **105**, 863-873.

Nowaczyk, M. J., Huggins, M. J., Tomkins, D. J., Rossi, E., Ramsay, J. A., Woulfe, J., Scherer, S. W. and Belloni, E. (2000). Holoprosencephaly, sacral anomalies, and situs ambiguus in an infant with partial monosomy 7q/trisomy 2p and SHH and HLXB9 haploinsufficiency. *Clin. Genet.* **57**, 388-393.

Oberdick, J., Wallace, J. D., Lewin, A. and Smeyne, R. J. (1994). Transgenic expression to monitor dynamic organization of neuronal development: use of the Escherichia coli lacZ gene product, β-galactosidase. *NeuroProtocols* **5**, 54-62.

Pepicelli, C. V., Lewis, P. M. and McMahon, A. P. (1998). Sonic hedgehog regulates branching morphogenesis in the mammalian lung. *Curr. Biol.* **8**, 1083-1086.

Qiao, J., Uzzo, R., Obara-Ishihara, T., Degenstein, L., Fuchs, E. and Herzlinger, D. (1999). FGF-7 modulates ureteric bud growth and nephron number in the developing kidney. *Development* **126**, 547-554.

Raatikainen-Ahokas, A., Hytonen, M., Tenhunen, A., Sainio, K. and Sariola, H. (2000). BMP-4 affects the differentiation of metanephric mesenchyme and reveals an early anterior-posterior axis of the embryonic kidney. *Dev. Dyn.* **217**, 146-158.

Saxen, L. (1987). *Organogenesis of the Kidney*. New York: Cambridge University Press.

St-Jacques, B., Dassule, H. R., Karavanova, I., Botchkarev, V. A., Li, J., Danielian, P. S., McMahon, J. A., Lewis, P. M., Paus, R. and McMahon, A. P. (1998). Sonic hedgehog signaling is essential for hair development. *Curr. Biol.* **8**, 1058-1068.

St-Jacques, B., Hammerschmidt, M. and McMahon, A. P. (1999). Indian hedgehog signaling regulates proliferation and differentiation of chondrocytes and is essential for bone formation. *Genes Dev.* **13**, 2072-2086.

Sukegawa, A., Narita, T., Kameda, T., Saitoh, K., Nohno, T., Iba, H., Yasugi, S. and Fukuda, K. (2000). The concentric structure of the developing gut is regulated by Sonic hedgehog derived from endodermal epithelium. *Development* **127**, 1971-1980.

Tacciuoli, M., Lotti, T., de Matteis, A. and Laurenti, C. (1975). Development of the smooth muscle of the ureter and vesical trigone: histological investigation in human fetus. *Eur. Urol.* **1**, 282-286.

Tanagho, E. A. (1981). Development of the ureter. In *The Ureter* (ed. H. Bergman), pp. 1-12. New York: Springer-Verlag.

Tanimoto, H., Itoh, S., ten Dijke, P. and Tabata, T. (2000). Hedgehog creates a gradient of DPP activity in Drosophila wing imaginal discs. *Mol. Cell* **5**, 59-71.

Valentini, R. P., Brookhiser, W. T., Park, J., Yang, T., Briggs, J., Dressler, G. and Holzman, L. B. (1997). Post-translational processing and renal expression of mouse Indian hedgehog. *J. Biol. Chem.* **272**, 8466-8473.

Wilkinson, D. G., Bailes, J. A., Champion, J. E. and McMahon, A. P. (1987a). A molecular analysis of mouse development from 8 to 10 days post coitum detects changes only in embryonic globin expression. *Development* **99**, 493-500.

Wilkinson, D. G., Bailes, J. A. and McMahon, A. P. (1987b). Expression of the proto-oncogene int-1 is restricted to specific neural cells in the developing mouse embryo. *Cell* **50**, 79-88.

Yang, Y., Relan, N. K., Przywara, D. A. and Schuger, L. (1999). Embryonic mesenchymal cells share the potential for smooth muscle differentiation: myogenesis is controlled by the cell's shape. *Development* **126**, 3027-3033.

Zambrowicz, B. P., Imamoto, A., Fiering, S., Herzenberg, L. A., Kerr, W. G. and Soriano, P. (1997). Disruption of overlapping transcripts in the ROSA beta geo 26 gene trap strain leads to widespread expression of beta-galactosidase in mouse embryos and hematopoietic cells. *Proc. Natl. Acad. Sci. USA* **94**, 3789-3794.